

## Cytotoxicity, anti-tumor effects and structure-activity relationships of nickel and palladium S,C,S pincer complexes against double and triple-positive and triple-negative breast cancer (TNBC) cells

Mahboubeh Hosseini-Kharat<sup>a,b</sup>, Rahmatollah Rahimi<sup>a,\*</sup>, Ali Mohammad Alizadeh<sup>b,c,\*</sup>, Davit Zargarian<sup>d,\*</sup>, Solmaz Khalighfard<sup>b</sup>, Loïc P. Mangin<sup>d</sup>, Nasim Mahigir<sup>a</sup>, Seyed Hasan Ayati<sup>e,f</sup>, Amir Abbas Momtazi-Borojeni<sup>g,h</sup>

<sup>a</sup> Department of Chemistry, Iran University of Science and Technology, Tehran 16846-13114, Iran

<sup>b</sup> Cancer Research Center, Tehran University of Medical Sciences, Tehran, Iran

<sup>c</sup> Breast Disease Research Center, Tehran University of Medical Sciences, Tehran, Iran

<sup>d</sup> Département de Chimie, Université de Montréal, Montréal, Québec H3C 3J7, Canada

<sup>e</sup> Immunology Research Center, Department of Immunology, Medical School, Mashhad University of Medical Sciences, Mashhad, Iran

<sup>f</sup> Department of Medical Immunology, Student Research Committee, Faculty of Medicine, Mashhad University of Medical Sciences, Mashhad, Iran

<sup>g</sup> Nanotechnology Research Center, Bu-Ali Research Institute, Mashhad University of Medical Sciences, Mashhad, Iran

<sup>h</sup> Department of Medical Biotechnology, Student Research Committee, Faculty of Medicine, Mashhad University of Medical Sciences, Mashhad, Iran

### ARTICLE INFO

#### Keywords:

TNBC  
Organometallic compounds  
Nickel  
Palladium  
Antitumor

### ABSTRACT

Triple-Negative Breast Cancer (TNBC) is a highly aggressive form of breast cancer. The high rate of metastasis associated with TNBC is attributed to its multidrug resistance, making the treatment of this metastatic condition difficult. The development of metal-based antitumor agents was launched with the discovery of cisplatin, followed by the development of related antitumor drugs such as carboplatin and oxaliplatin. Yet, the severe side effects of this approach represent a limitation for its clinical use. The current search for new metal-based antitumor agents possessing less severe side effects than these platinum-based complexes has focused on various complexes of nickel and palladium, the group 10 congeners of platinum. In this work, we have prepared a series of SCS-type pincer complexes of nickel and palladium featuring a stable meta-phenylene central moiety and two chelating but labile thioamide donor moieties at the peripheries of the ligand. We have demonstrated that the complexes in question, namely  $L^1NiCl$ ,  $L^1NiBr$ ,  $L^1PdCl$ ,  $L^2PdCl$ , and  $L^3PdCl$ , are active on the proliferation of estrogen-dependent breast tumor cells (MCF-7 and MC4L2) and triple-negative breast cancer (4 T1). Among the complexes studied, the palladium derivatives were found to be much safer anticancer agents than nickel counterparts; these were thus selected for further investigations for their effects on tumor cell adhesion and migration as well. The results of our studies show that palladium complexes are effective for inhibiting TNBC 4 T1 cells adhesion and migration. Finally, the HOMO and LUMO analysis was used to determine the reactivity and charge transfer within the compounds.

Breast cancer (BC) is the most common cancer in women worldwide and the second most common cancer overall<sup>1</sup>. Immunohistochemical (IHC) analysis of the tumor expression has revealed three breast cancer subtypes: estrogen/progesterone dependent (ER/PR+), the epidermal growth factor 2 dependent (HER2+) and Triple-Negative Breast Cancer (TNBC)<sup>2</sup>. The latter, TNBC, which lacks the expression of all three receptors (ER, PR and HER2), is a highly aggressive breast cancer subtype that is responsible for about 20% of breast cancers. The high rates of

metastasis in these cells is associated with the fact that they frequently display multidrug resistance, thus complicating the treatment of this metastatic effect<sup>3-4</sup>. The pattern of metastatic spread in TNBC is different from other breast cancer subtypes, frequently resulting in a higher likelihood of brain and lung cancer, and less frequently bone lesions<sup>5</sup>. In addition, no specific chemotherapy agent is able to cease metastatic spread, and most patients with TNBC die from advanced disease within 20 months post progression<sup>5,6</sup>.

\* Corresponding authors.

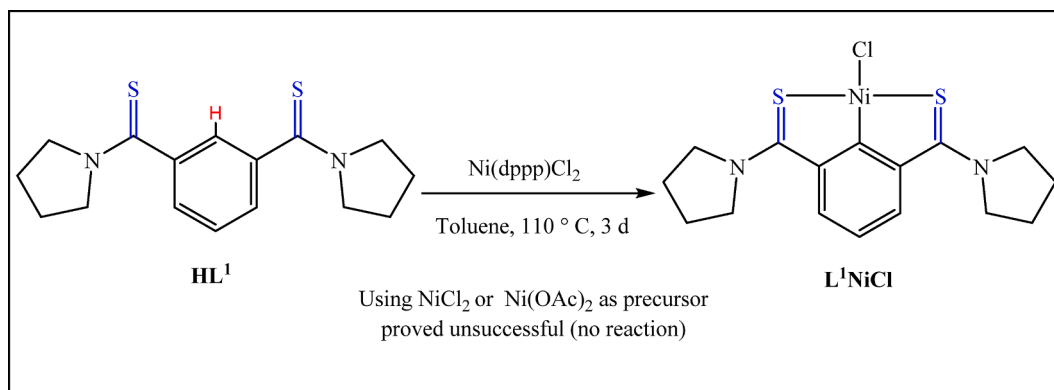
E-mail addresses: [rahimi\\_rah@iust.ac.ir](mailto:rahimi_rah@iust.ac.ir) (R. Rahimi), [aalizadeh@sina.tums.ac.ir](mailto:aalizadeh@sina.tums.ac.ir) (A.M. Alizadeh), [zargarian.davit@umontreal.ca](mailto:zargarian.davit@umontreal.ca) (D. Zargarian).

<https://doi.org/10.1016/j.bmcl.2021.128107>

Received 9 February 2021; Received in revised form 4 May 2021; Accepted 10 May 2021

Available online 13 May 2021

0960-894X/© 2021 Published by Elsevier Ltd.



**Scheme 1.** Synthesis of pincer complex  $\text{L}^1\text{NiCl}$ .

Cisplatin and its derivatives, oxaliplatin and carboplatin, are the only metal-based chemotherapeutic drugs approved for worldwide clinical practice. They have been used and are effective for the treatment of numerous human cancers. However, cisplatin has been reported to cause drug resistance and several undesirable side effects such as allergic reactions, decreased immunity to infections, severe kidney problems, gastrointestinal disorders, haemorrhage, and hearing loss<sup>7,8</sup>. All these shortcomings have motivated extensive investigations into alternative metal-based cancer therapies that effectively target both cancer cell proliferation and metastasis.

In this context, it has been shown that studying anticancer activity of non-platinum metal-based complexes (NPMBC) as chemotropic agents is of great importance. For instance, it has been demonstrated that NPMBC, besides enhancing the potential of anticancer therapies, can be used as monotherapy to prevent cancer cell migration, invasion and/or metastasis<sup>8–11</sup>. These findings were confirmed by Paholak et al.<sup>12</sup> using an in vivo model.

In another study, Biancalana et al.<sup>13</sup> observed that ruthenium complexes have good cytotoxic activity, with  $\text{IC}_{50}$  values substantially lower than the values obtained with cisplatin on MDA-MB-231 cells. These differences could be due to having different mechanisms of action; for instance, cisplatin and ruthenium-based complexes might differ in the activation of p53-dependent or p53-independent checkpoints<sup>14–17</sup>. Since platinum-based drugs and NPMBC act on different pathways, NPMBC could lead to entirely new therapeutic options for patients with TNBC resistant to platinum-based drugs.

Of great relevance to this topic, many bioactive sulfur-containing compounds have displayed protective effects against different types of cancer. More interestingly, they are reported as radical scavengers for protecting cells from free radicals<sup>18</sup>. Sulfur-containing compounds also interact easily with reactive oxygen species (ROS) owing to their strong nucleophilic property<sup>19</sup>. Thus, the thiol radical fragment is very important for radical scavenging and anti-proliferative effects of these family of compounds.

The above-mentioned points have spurred us to rationally design metal-based and sulfur-containing complexes that might possess anticancer properties. In our previous works, we prepared a family of nickel complexes featuring SCS thioamide-based pincer ligands<sup>20–21</sup>. We showed that the thioamide-bearing pre-ligands react with the nickel precursor via C–H metallation to give nickel complexes chelated by a tridentate pincer-type ligand and adopting an approximately square planar geometry. This study also examined the antiproliferative activity of these nickel complexes against hormone responsive breast cancer cells. Our results showed that the nickel compounds had promising antitumor activity in vitro, as well as in vivo administration of the compound containing iodide ligand and pyrrolidine component in the thioamide moieties. These compounds significantly inhibited tumor growth in the estrogen-dependent MC4L2 cancer cells in female BALB/c mice. We posited that the coordination geometry imposed by the SCS

ligand played a pivotal role in the biological behavior of the complex. Indeed, preliminary studies showed that the planar geometry of these compounds are beneficial for promoting drug-DNA intercalation.

The present study presents a comparison of closely related SCS-type pincer complexes of nickel bearing different halide ions, chloride and bromide. It is known that halide ions play a critical role in regulating the activities of metal-based drugs. For instance, the interaction between cisplatin and DNA is related to the presence of labile chloride ions that can be exchanged for water molecules, hence forming an electrophilic complex<sup>22</sup>. This leads to the platinum ion interacting with DNA at the N7 positions of either two guanine or guanine and adenine bases, hindering DNA replication and can inhibit transcription. In view of the major role played by halide ions in the mechanism of preventing tumor progress, we set out to compare antitumor effects of nickel complexes with various halides (chloride, bromide and iodide).

A second focus of the present study is on palladium-based anticancer therapeutics. Palladium is very similar to platinum in both its chemical and physical properties. Thanks to this similarity, palladium compounds have been regarded as a good alternative for platinum antitumor drugs for decreasing severe side effects of cisplatin and its family of complexes. In general, palladium complexes are less toxic than their platinum counterparts. For example,  $\text{LD}_{50}$  (median lethal dose) of platinum chloride administered orally in rats is 276 mg/kg, while this figure is 2704 mg/kg for palladium, representing a tenfold lower toxicity for the Pd salt<sup>22</sup>. The lower toxicity of the palladium compounds leads to less severe side effects. Many palladium-based anticancer drugs have been prepared with sulfur donor ligands, since sulfur-containing compounds have also been shown to reduce nephrotoxicity<sup>23</sup>.

Therefore, we have prepared a family of palladium complexes featuring thioamide ligands for the sake of their activity against different breast cancer types. It is worth noting that existing chelating ligands promoting metallacycle formation are privileged, as these factors can stabilize palladium ions, thus reducing their lability in physiological media. It is worth emphasizing that to date no account has been published on biological activity and anticancer effect of SCS palladium complexes. We believe that palladium ions featuring planar geometry and S-donor ligands will have a great impact on the antitumor potency of Pd pincer complexes in this project. Therefore, the aim of this work is to compare the activities of structurally similar nickel and palladium complexes on healthy cells and different types of hormone responsive and non-responsive breast tumor cells and, after identifying the more cytotoxic complexes, to further investigate their effects on TNBC cell adhesion and migration in vitro. MCF-7, MC4L2 and 4 T1 are the three cell lines that are treated with nickel and palladium complexes as anticancer agents here. MCF-7 is a double positive human breast cancer (ER/PR+ and HER2–). MC4L2 is a triple-positive mouse breast cancer cell line (ER/PR/HER2+) and 4 T1 is a triple-negative mouse breast cancer cell line (ER/PR/HER2–).

The synthetic methodology used for the preparation of the  $\text{L}^1\text{NiCl}$

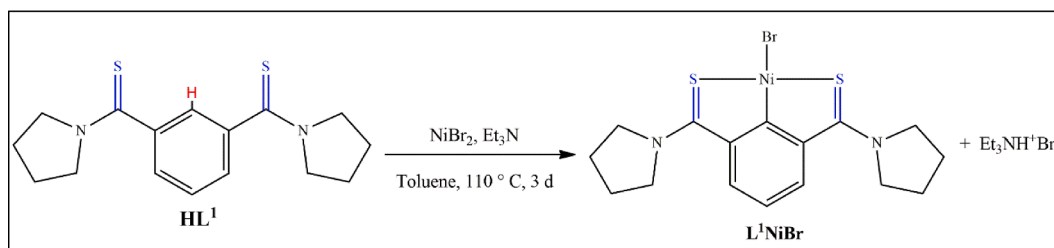
Scheme 2. Synthesis of pincer complex  $L^1NiBr$ .

Table 1

Electronic spectral data of  $HL^1$ ,  $L^1NiCl$  and  $L^1NiBr$ .

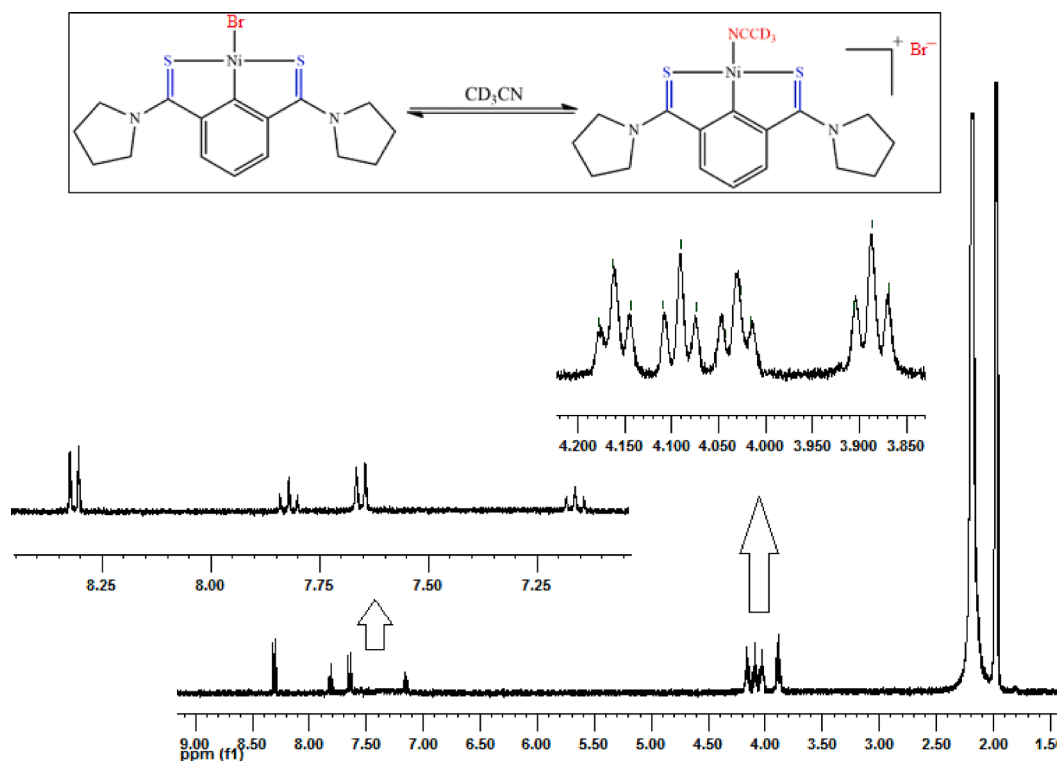
Compound	$\lambda_{max}$ (nm)	$\epsilon$ (Lmol <sup>-1</sup> cm <sup>-1</sup> )	Assignment
$HL^1$	230	40,477	$\pi \rightarrow \pi^*$
	285	29,883	$n \rightarrow \pi^*$
$L^1NiCl$	249	94,230	LC
	475	9725	$d \rightarrow d$
$L^1NiBr$	249	60,883	LC
	475	6706	$d \rightarrow d$

and  $L^1NiBr$  via C–H nickelation is shown in Schemes 1 and 2. The SCS proligand  $HL^1$  was synthesized by the Willgerodt–Kindler reaction described in the previous publication<sup>24</sup>. An initial effort for the preparation of both complexes was unsuccessful. Unlike the metallation reaction of this ligand with  $NiI_2$  precursor<sup>21</sup>, preparing chloride and bromide counterparts was more challenging and required optimized reaction conditions. Initial attempts involving the use of precursors such as anhydrous  $NiCl_2$  or  $Ni(OAc)_2$  proved unsuccessful, regardless of whether the reactions were carried out (a) in the presence or absence of triethylamine ( $NEt_3$ ), (b) using polar or non-polar solvents, and (c) at room temperature or with heating. Optimization studies indicated that the crucial factor in the synthesis was the use of the nickel precursor  $Ni(dppp)Cl_2$  ( $dppp$  = 1,3-bis(diphenylphosphino)propane). Using this

precursor, the C–H nickelation reaction proceeded smoothly to give the SCS-type complex  $L^1NiCl$ . (Scheme 1). The reason for this is likely that  $dppp$  is playing the role of base here, absorbing the  $HCl$  generated in the reaction. Moreover, with  $dppp$ , we have a monomer that reacts more easily, whereas with  $NiCl_2$  we have a polymer and the pincer ligand is not able to break it up easily.

Interestingly, the synthesis of the bromo analogue  $L^1NiBr$  proceeded by stirring  $HL^1$  with  $NiBr_2$ , but in this case  $NEt_3$  was required to promote the C–H nickelation step (Scheme 2). As mentioned above, we have reported the synthesis route of iodo analogue  $L^1NiI$  previously.<sup>21</sup> Comparisons between  $L^1NiCl$ ,  $L^1NiBr$  and  $L^1NiI$ , show that the latter complex is straightforwardly synthesized without the presence of a base. The difference between halide analogues may be attributed to the stronger Ni-halide bond which diminishes the formation of the C–Ni bond.

$L^1NiCl$  and  $L^1NiBr$  are stable in ambient atmosphere (moist air) and show good solubility in organic solvents such as  $CH_2Cl_2$ ,  $CHCl_3$ , DMF, and DMSO. Full characterization of both complexes was accomplished by  $^1H$  NMR,  $^{13}C\{^1H\}$  NMR, IR, UV–vis spectroscopies and elemental analysis. The IR spectra of both complexes show that the  $\nu(C-N)$  for the thioamide group has shifted to higher frequencies relative to the free ligand (1508 vs 1498  $cm^{-1}$ , which implies a moderate reinforcement of the C–N interaction in  $L^1NiCl$  and  $L^1NiBr$  as a result of S-coordination of the thioamide group<sup>24</sup>. Furthermore, the  $\nu(C-S)$  vibrational

Fig. 1.  $^1H$  NMR spectrum of  $L^1NiBr$  showing the equilibrium reaction with solvent.

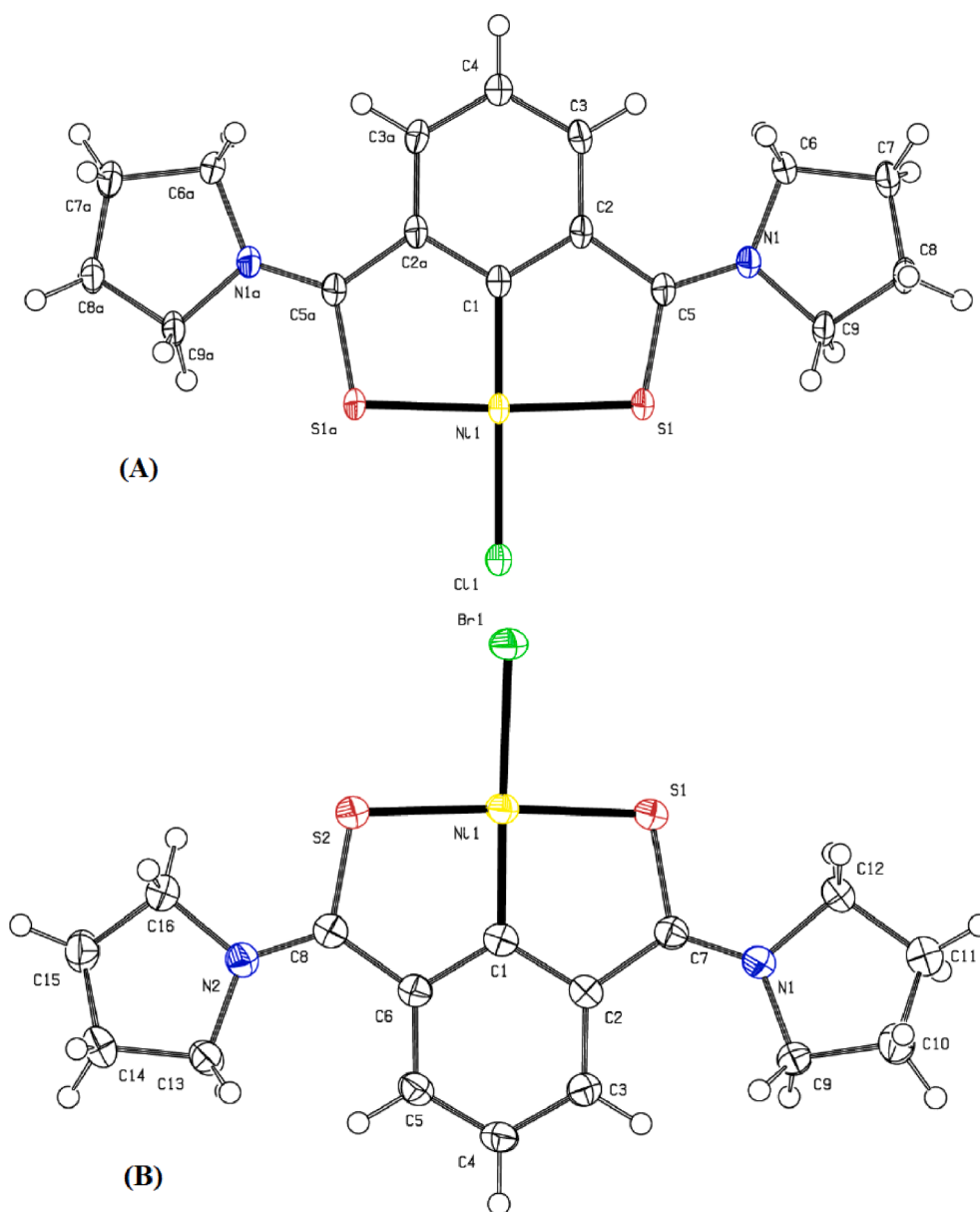


Fig. 2. The molecular structure of  $L^1NiCl$  (A) and  $L^1NiBr$  (B) with displacement ellipsoids drawn at the 50% probability level.

frequencies assigned to the stretching and bending modes of complexes were observed at  $1170\text{--}1174\text{ cm}^{-1}$  and  $615\text{ cm}^{-1}$ , respectively, relative to the corresponding free ligand values  $1170$  and  $709\text{ cm}^{-1}$ .<sup>25,26</sup>

Both complexes exhibit an intense electronic absorption band at  $\lambda_{\text{max}}$   $249\text{ nm}$  in their UV-vis spectra (Fig. S1 and Table 1), which is assigned to the LC (ligand-centered) transition in the  $HL^1$ .<sup>27</sup> Moreover, they show absorption at about  $475\text{ nm}$  ascribed to a d-d transition ( $^1A_{1g} \rightarrow ^1A_{2g}$ ). The low energy band is typical of d-d transition in square planar Ni(II) complexes with a mixed coordination sphere containing nitrogen, oxygen, and sulfur atoms.<sup>28</sup> The  $^1H$  NMR spectra of the complexes (Fig. 1) document the disappearance of the signal for C2-H of the central benzene ring. The  $^{13}C\{^1H\}$  NMR spectra also provide support for the C-H nickelation at the C2 position: a significant downfield shift is noted for the C2 carbon resonance relative to the corresponding resonance in the free proligand  $HL^1$  ( $\delta$   $145.1\text{--}147.0\text{ ppm}$  vs.  $\delta$   $128.5\text{ ppm}$ ). The impact of the interaction between the Ni center and the aryl moiety is also apparent in significant shifts in the  $^{13}C$  resonances of the aromatic ring.<sup>24</sup> It is also worth noting that these spectra show two sets of signals in the aliphatic and aromatic regions for  $L^1NiBr$ , indicating two species

involved in dynamic exchange.<sup>21,29–32</sup> This is thought to arise from the equilibrium displacement of the labile halides by the fairly nucleophilic solvent  $CD_3CN$ , thus forming in-situ generated cationic complexes. Finally, the  $^{13}C$  signals appearing downfield of  $\delta$   $195\text{ ppm}$  are ascribed to the thioamide carbon ( $C=S$ ) in these complexes.

Fig. 2 illustrates the solid state structures of  $L^1NiCl$  and  $L^1NiBr$ , assigned by X-ray crystallography; the crystallographic data and selected bond lengths and angles of the complexes are summarized in Tables S1 and S2, respectively. The asymmetric unit in the crystal structure of  $L^1NiCl$  consists of half a molecule, for which the full molecule is generated by a  $C_2$  symmetry axis. In the packing diagrams of complexes, adjacent molecules are connected to each other via  $CH\cdots\pi$  and  $CH\cdots S$  interactions (Fig. 3 and Fig. S2).

As shown in the molecular diagrams, the nickel(II) center in both complexes is bonded to a meridional, tridentate SCS pincer ligand forming two symmetrical 5-membered metallacycle rings. In both cases, sum of the bond angles around the Ni(II) center is ca.  $360^\circ$ , indicating a nearly ideal square planar molecular geometry. On the other hand, there is a slight tilting of the central benzene ring out of the coordination

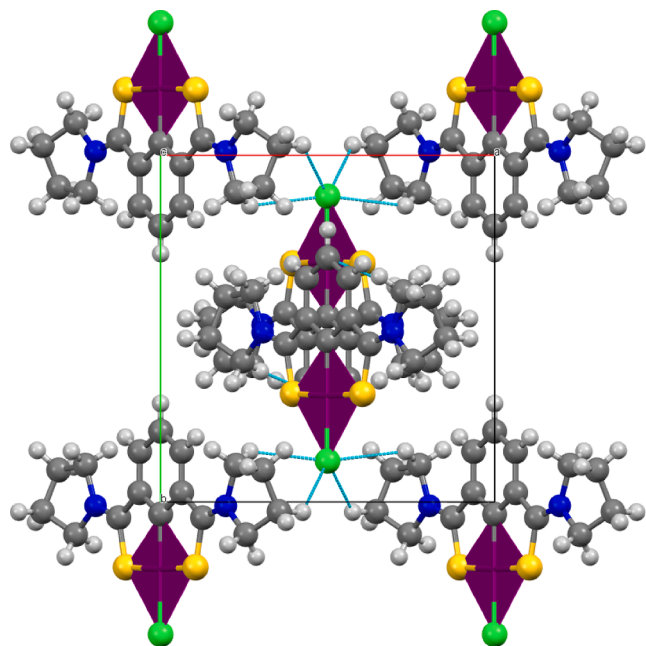


**Fig. 3.** Packing diagram of  $L^1NiCl$  along with  $b$  axis. Adjacent molecules are connected with  $CH\cdots\pi$  interactions.  $CH\cdots S$  interaction is also observed among neighboring molecules.

**Table 2**

$IC_{50}$  values ( $\mu M$ ) of different SCS nickel and palladium complexes against various breast cancer and healthy cells with exposure time of 48 h. The cytotoxic activity of cisplatin was evaluated at the same condition as a standard reference.

	MC4L2	4 T1	MCF7	MF
$L^1NiCl$	N.D	$19 \pm 0.60$	$25 \pm 0.10$	$>100$
$L^1NiBr$	N.D	$65 \pm 0.20$	$26 \pm 0.01$	$>100$
$L^1NiI$	N.D	$40 \pm 0.04$	$40 \pm 0.01$	$>100$
$L^2NiI$	N.D	$40 \pm 0.01$	$40 \pm 0.01$	$>100$
$L^3NiI$	N.D	$40 \pm 0.03$	$40 \pm 0.01$	100
$L^4NiI$	N.D	$100 \pm 0.01$	$200 \pm 0.09$	$>100$
$L^1PdCl$	$40 \pm 0.03$	$40 \pm 0.07$	$100 \pm 0.01$	$>200$
$L^2PdCl$	$20 \pm 0.23$	$20 \pm 0.04$	$20 \pm 0.01$	$>200$
$L^3PdCl$	$100 \pm 0.07$	$100 \pm 0.03$	$40 \pm 0.41$	$>200$
cisplatin	$10 \pm 0.01$	$17 \pm 0.08$	$12 \pm 0.30$	$10 \pm 0.50$

plane, as reflected by the angle between this ring and the SCS plane:  $2.38^\circ$  ( $L^1NiCl$ ) and  $3.78^\circ$  ( $L^1NiBr$ ). The  $Ni1-Cl1$  and  $Ni1-Br1$  bond lengths are  $2.2262(5)$  and  $2.3643(9)$  Å, respectively, which are smaller than the reported  $Ni1-I$  bond length ( $2.5620(7)$  Å) in  $L^1NiI$ .<sup>21</sup>

Moreover, the  $Ni-C_{(aryl)}$  bond lengths in two SCS complexes are  $1.873(2)$  Å ( $L^1NiCl$ ), and  $1.863(5)$  Å ( $L^1NiBr$ ). These are within range of the corresponding distances reported for nickel SCS complexes,<sup>21</sup> as well as *m*-phenylene-based nickel PCP pincer and C,P cyclonickellated complexes ( $1.880(2)$ – $1.931(2)$ ),<sup>33–35</sup> but longer than in the recently published nickel NCN pincer complexes ( $1.822(2)$ – $1.825(5)$ ).<sup>36</sup>

To evaluate the in vitro cytotoxicity of the nickel complexes, the triple-negative 4 T1 and the estrogen-responsive MCF-7 breast cancer cell lines were exposed to each of the  $L^1NiCl$  and  $L^1NiBr$  at the concentrations of  $10 \mu M$  to  $100 \mu M$  for 48 h. The MTT-dye reduction method was employed to determine the half-maximal inhibitory concentration ( $IC_{50}$ ) of the complexes. The cytotoxic activity of cisplatin, a standard anti-cancer drug, was evaluated under the same experimental conditions for comparison purposes. Both nickel complexes displayed good cytotoxicity against 4 T1 and MCF-7 breast cancer cells; they also showed low toxicity ( $IC_{50}$  values  $>100 \mu M$ ) on MF normal cells when compared with cisplatin.

As shown in Fig. S3, the compounds display concentration-

dependent cytotoxicity against both cancer cell lines.  $L^1NiBr$  has potent cytotoxic activity against 4 T1 and MCF-7 cancer cell lines with  $IC_{50}$  values of  $65 \mu M$  and  $26 \mu M$ , respectively (Table 2). Higher cytotoxic activity was observed on 4 T1 and MCF-7 cancer cell lines treated by  $L^1NiCl$  with  $IC_{50}$  values of  $19 \mu M$  and  $25 \mu M$ , respectively. Thereby, the latter exerted high cytotoxicity on both estrogen-responsive and unresponsive breast cancer. The reason for this may be attributed to the structure of  $L^1NiCl$ . As crystallographic data have shown, this compound possesses a regular square planar geometry without any deviation, making the complex ideally suited for potential intercalation into DNA, which is likely to result in enhanced antitumor activity.

We evaluated the cytotoxicity of three palladium(II) complexes ( $L^1PdCl$ ,  $L^2PdCl$  and  $L^3PdCl$ ) against three breast cancer cells: hormone-responsive (MCF7), triple-positive (MC4L2) and triple-negative (4 T1). These complexes possess structures based on tridentate thioamide ligands with pyrrolidine, piperidine and morpholine moieties (Fig. 4). All three breast cancer cells were incubated with different doses of the palladium complexes ( $5$ – $200 \mu M$ ) with different exposure times (24, 48, and 72 h). As was the case for the nickel complexes, the cytotoxic activity of cisplatin was evaluated under the same conditions as a standard reference for comparison purposes.  $IC_{50}$  values were calculated from curves constructed by plotting cell viability (%) versus compound concentration ( $\mu M$ ) (Fig. S4).

The results indicated that reduction of cancer cell viability for three complexes is time- and dose-dependent, and cell death has increased with growing compound concentrations (Table 3). One striking point is that  $L^2PdCl$  containing piperidine moiety was almost more cytotoxic among three complexes in the aforementioned times. In addition,  $L^2PdCl$  and  $L^3PdCl$  are complexes that are effective at a short exposure time of 24 h. The activity of  $L^3PdCl$  at this time could be attributed to the existing of morpholine rings in its structure, it seems that the presence of oxygen in the morpholine unit may exert influence on its antitumor activity. One likely reason for this behavior may be the participation of oxygen in donor–acceptor type interactions with the substrate, i.e., formation of a strong complex with its target.<sup>37</sup> For instance, it can engage in H-bonding with the amino acid residues and nucleotides in protein and DNA of damaged cells, and this may accelerate denaturation of their structures in the cancerous cells. Further studies such as DNA-binding analysis are needed to determine the antitumor mechanism of complexes. Our previous study<sup>20</sup> has shown that complex  $L^3NiI$  binds to DNA by non-covalent interaction, broadly through the intercalation mode. We estimate that due to the almost flat square structure of the complexes, one of the possible mechanisms of interaction with DNA could be the intercalation binding.

Finally, the cytotoxic activity of the complexes and cisplatin on normal cells MF has been assayed and the results indicated that all palladium complexes have lower cytotoxic effect on normal cells amid complexes as well as cisplatin in different exposure times. As was mentioned earlier, antitumor effect of SCS-nickel and -palladium complexes has received little attention in the literature. Indeed, to our knowledge, this study is the first account of antitumor activity of SCS palladium complexes. Churusova et al.<sup>38</sup> reported the preparation of the structurally related NNS- and NNN-type pincer complexes of palladium based on carboxamide ligands functionalized with amino acids. These compounds have been examined against a variety of cancer cells including MCF7 breast cancer and exhibited the range of  $IC_{50}$  values between  $5.5$  and  $22.0 \mu M$  which is comparable with our results.

Furthermore, their comparative studies determined that the presence of the sulfide ancillary donor group is crucial for cytotoxic activity of this type of Pd(II) complexes. In another study, the SNO-type tridentate pincer palladium complexes with isatin-based thiosemicarbazone ligands have been reported to inhibit proliferation of human breast (MCF7) cancer cells in vitro. The obtained  $IC_{50}$  values were in the range of  $22.36$ – $53.37 \mu M$  with a short 24 h incubation period.<sup>39</sup>

Since many factors can influence the activity of metal complexes, it may be difficult to define straightforward structure–activity



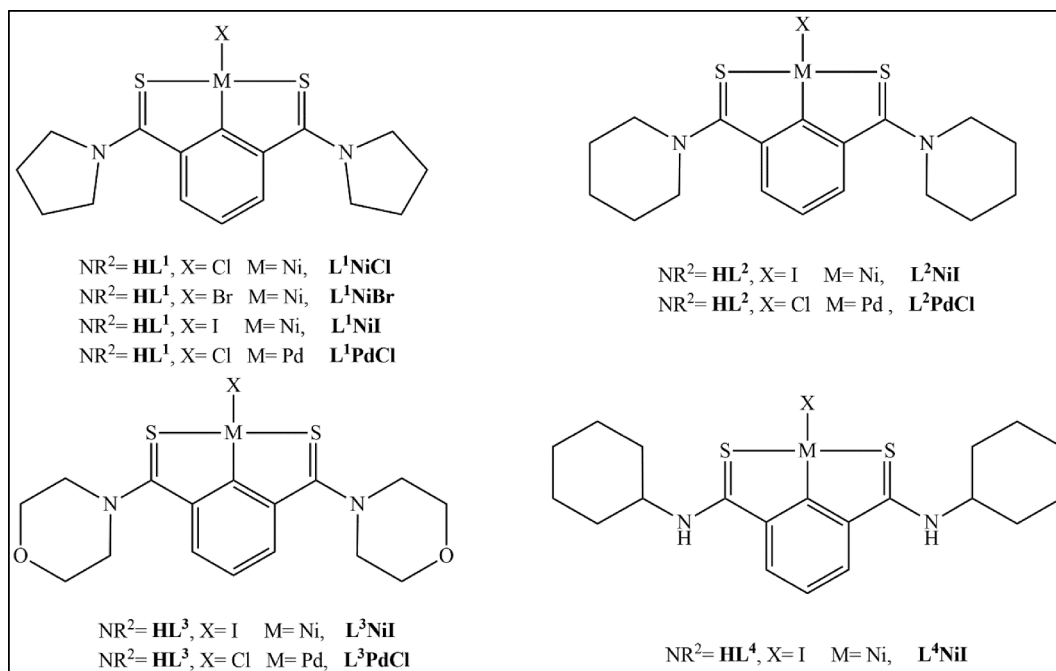


Fig. 4. List of nickel and palladium SCS complexes screened for antitumor activity.

Table 3

IC<sub>50</sub> values (μM) obtained for **L<sup>1</sup>PdCl**, **L<sup>2</sup>PdCl** and **L<sup>3</sup>PdCl** against various breast cancer and healthy cell lines with different exposure times.

IC <sub>50</sub> (μM)		Breast cancer cells Complex		
		72 h	48 h	24 h
40 ± 0.33	100 ± 0.01	>200	MCF7	<b>L<sup>1</sup>PdCl</b>
20 ± 0.21	40 ± 0.03	>200	MC4L2	
20 ± 0.05	40 ± 0.07	>200	4 T1	
>200	>200	>200	MF	
10 ± 0.06	20 ± 0.01	200	MCF7	<b>L<sup>2</sup>PdCl</b>
10 ± 0.05	20 ± 0.23	200	MC4L2	
10 ± 0.02	20 ± 0.04	200	4 T1	
>200	>200	>200	MF	
10 ± 0.01	40 ± 0.41	200 ± 0.03	MCF7	<b>L<sup>3</sup>PdCl</b>
10 ± 0.03	100 ± 0.07	200 ± 0.02	MC4L2	
10 ± 0.06	100 ± 0.03	200 ± 0.31	4 T1	
>200	>200	>200	MF	

relationships describing promising anticancer agents. However, some tentative conclusions can be drawn from the in vitro studies of the title nickel and palladium complexes, which could be helpful in further work

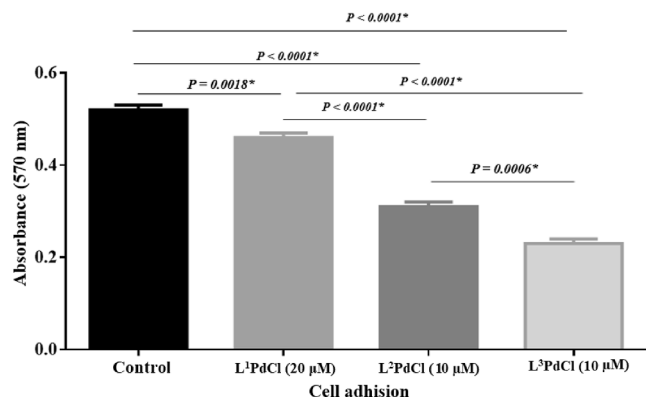


Fig. 5. Result of the cell adhesion assay at 570 nm. Effect of palladium complexes on the cell adhesion against TNBC 4 T1 cell line.

on the design of new tumor active metal complexes. We tabulated IC<sub>50</sub> values of nine SCS nickel and palladium complexes as well as cisplatin against various breast cancer and healthy cells with an exposure time of 48 h (Table 2). Some data of the table have been taken from our previous publications<sup>20,21</sup> and we reported them for comparison. As mentioned above, the amine moieties present in the skeleton of the SCS-type pincer ligands, namely pyrrolidine, piperidine, morpholine, and cyclohexylamine (Fig. 4), appear to play an important role in the biological properties probed in the present study. The highlights of our findings from the antitumor activity of various nickel and palladium complexes based on S,C,S type pincer ligands are listed below:

- (1) Among the **L<sup>1</sup>Ni** complexes with various halide ions, the largest cytotoxicity on double-positive breast cancer MCF7 cells belongs to **L<sup>1</sup>NiCl** and the cytotoxicity ratio is as follows: **L<sup>1</sup>NiCl** > **L<sup>1</sup>NiBr** > **L<sup>1</sup>NiI**. It has been established that the leaving group LG has a pivotal role in the drug pharmacokinetics, allowing the metal antitumor agent to reach its target and to get activated by hydrolysis with the exchange of LG labile ligands with water molecules.<sup>40</sup> In this regard, the water solubility of the complex is an important issue that can modulate the toxicity of the drug.
- (2) Palladium complexes showed the lowest toxicity on healthy cells among the studied compounds, which is an advantage. They could be considered as safe antitumor agents.
- (3) Various IC<sub>50</sub> values were obtained against different types of breast cancer cells using the same complex. It shows that in addition to the molecular structure of the complex, the structure of tumor cells is also effective.
- (4) **L<sup>4</sup>NiI** containing cyclohexylamine fragment displayed moderate cytotoxic activity among all complexes. It seems that the high steric hindrance of the amine fragment causes a decrease in cytotoxic activity. Similar behavior has been reported for some platinum complexes, in which steric effects resulted in diminishing of binding to DNA and therefore declining the antitumor activity.
- (5) Comparisons between nickel and palladium complexes showed that they showed almost the same anticancer properties against different cancer cells and there is not much difference between

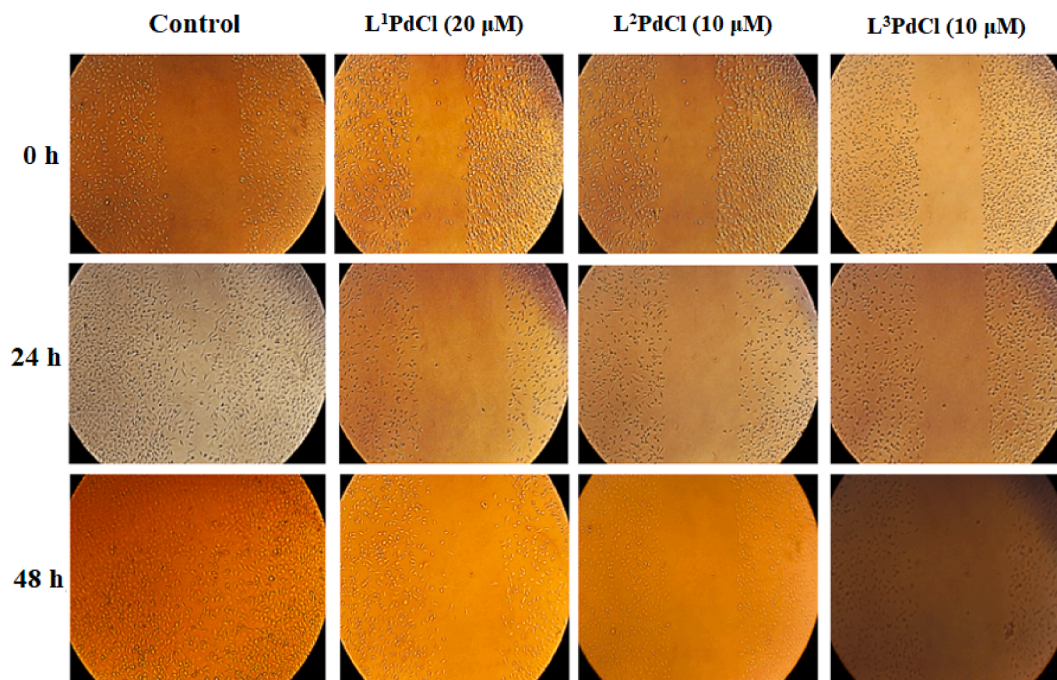


Fig. 6. Results of the scratch-wound assay. Effect of palladium complexes on cell migration against TNBC 4 T1 cell line.

their outcomes. However, we might expect nickel complexes to be more active because of the presence of labile  $\text{Ni}^{2+}$ . But due to the formation of the metallacyclic part, which renders greater stability for the complex, this expectation is reduced.

Cancer metastasis is a process in which cancer cells disseminate from the primary tumor, resulting in the formation of secondary tumors. The properties of cell adhesion and migration are fundamental in regulating cell movement and cancer metastasis and are necessary for the cells to move into the bloodstream. Since the palladium complexes manifested promising antitumor activity against various breast cancer cell lines and showed lower activity on healthy cells, they were chosen for further investigation and their anticancer activity were measured by adhesion and migration of cancer cells. The effect of these complexes on cell adhesion and migration was carried out at  $\text{IC}_{50}$  values on triple-negative breast cancer 4 T1 cell line. We selected TNBC since the remediation of this type of breast cancer is a challenging task among various other types. As shown in Fig. 5, three complexes inhibited cell adhesion by about 11.5% ( $\text{L}^1\text{PdCl}$ ), 28.8% ( $\text{L}^2\text{PdCl}$ ) and 42.3% ( $\text{L}^3\text{PdCl}$ ) with respect to the control. Evidently, the latter Pd(II) complex containing morpholine ligand remarkably mitigated cell adhesion; consequently, it is able to affect the metastatic potential of cancer cells by inhibiting their adhesion property. The effect of palladium complexes on 4 T1 cell migration was also evaluated using the in vitro scratch-wound assay. The studies on cancer cell migration were also accomplished considering the  $\text{IC}_{50}$  values used in cell adhesion assay. The confluence monolayer of 4 T1 cells was scratched and incubated in the presence or absence of palladium complexes (10–20  $\mu\text{M}$ ) for 24 and 48 h. Fig. 6 shows that treatment with all palladium complexes reduced the spreading of the 4T1 cells along the edges of the wound compared to an untreated control.

HOMO and LUMO energies are the most important descriptors for describing the drug-receptor interaction of the molecules. The small energy gap between HOMO and LUMO permits the transfer and exchange of electrons, causing an increase in the reactivity of the compounds. The calculations showed that the charge distribution of the HOMO level of nickel and palladium complexes mostly localized on the Ni(II) or Pd(II) center, sulfur atoms and halide ions. On the other hand,

Table 4  
MO energies, energy band gaps and dipole moments of the complexes.

Complex	$E_{\text{HOMO}}$ (eV)	$E_{\text{LUMO}}$ (eV)	$\Delta E$ (eV)	DM (Debye)
$\text{L}^1\text{NiCl}$	−0.2806	−0.0364	0.2442	16.0200
$\text{L}^1\text{NiBr}$	−0.2816	−0.0360	0.2456	16.1256
$\text{L}^1\text{NiI}$	−0.2672	−0.0347	0.2325	14.4199
$\text{L}^2\text{NiI}$	−0.2690	−0.0382	0.2308	13.5847
$\text{L}^3\text{NiI}$	−0.2783	−0.0485	0.2298	12.7544
$\text{L}^4\text{NiI}$	−0.2820	−0.0504	0.2316	12.4760
$\text{L}^1\text{PdCl}$	−0.2734	−0.0367	0.2367	17.5293
$\text{L}^2\text{PdCl}$	−0.2743	−0.0404	0.2339	16.3552
$\text{L}^3\text{PdCl}$	−0.2836	−0.0503	0.2333	15.7533

Table 5  
Electronic descriptors calculated from DFT calculations.

Complex	I (eV)	A (eV)	$\omega$ (Debye/V)	$\eta$ (eV)	$\mu$ (eV)
$\text{L}^1\text{NiCl}$	0.2806	0.0364	0.1028	0.1221	−0.1585
$\text{L}^1\text{NiBr}$	0.2816	0.0360	0.1026	0.1228	−0.1588
$\text{L}^1\text{NiI}$	0.2672	0.0347	0.0979	0.1162	−0.1509
$\text{L}^2\text{NiI}$	0.2690	0.0382	0.1022	0.1154	−0.1536
$\text{L}^3\text{NiI}$	0.2783	0.0485	0.1161	0.1149	−0.1634
$\text{L}^4\text{NiI}$	0.2820	0.0504	0.1192	0.1158	−0.1662
$\text{L}^1\text{PdCl}$	0.2734	0.0367	0.1015	0.1183	−0.1550
$\text{L}^2\text{PdCl}$	0.2743	0.0404	0.1058	0.1169	−0.1573
$\text{L}^3\text{PdCl}$	0.2836	0.0503	0.1194	0.1166	−0.1669

the LUMO electrons are largely localized on the CS–N group and aryl moiety with partial localization on the Ni(II) or Pd(II) center (Table S3). For understanding the biological efficiency of the compounds under study, different chemical reactivity descriptors have been calculated here. They include  $E_{\text{HOMO}}$ ,  $E_{\text{LUMO}}$ , the energy gap between these two ( $\Delta E$ ), the dipole moment (DM), ionization energy (I), electron affinity (A), chemical potential ( $\mu$ ), the hardness ( $\eta$ ) and the global electrophilicity power ( $\omega$ ). Numerical values for selected descriptors are listed in Tables 4 and 5. The calculations showed that the values of  $\Delta E$  for all compounds are almost in the same range. Yet, these figures for  $\text{L}^1\text{NiCl}$  and  $\text{L}^1\text{NiBr}$  are a bit higher than others reflecting their lower reactivity. The chemical potential ( $\mu$ ) of all compounds is negative and it means

that they are stable. The polarity of the molecule is generally expressed in terms of DM, and polar molecules dissociating better than non-polar molecules. As can be seen from Table 4, L1PdCl has the highest DM. The global hardness of  $L^1NiCl$  and  $L^1NiBr$  is the most. The hardness indicates the resistance towards the deformation of the electron cloud of chemical systems under small perturbation encountered during the chemical process.<sup>41</sup> The global electrophilicity power measures the stabilization in energy when the system acquires an additional electronic charge from the environment.  $L^3NiI$  has the lowest  $\omega$ .

In conclusion, this report has examined different reaction conditions for promoting the C—H nickelation of the thioamide-based SCS ligands. The nickel and palladium complexes obtained from the chelation of these ligands ( $(HL^1-HL^4)$ ) were then investigated against hormone-responsive and triple-negative breast cancer cells. Our findings revealed that cytotoxicity of compounds prepared here is dependent on the nature of central metal and different amine moieties in the structure of SCS ligands. For example, the palladium complex with piperidine moiety is more active among all other complexes. Taken together, the results show that palladium complexes are safer anticancer agents than nickel complexes. They also inhibit TNBC 4 T1 cell proliferation, adhesion, and migration. Also, this work supports the evidence that palladium complexes should be further studied to explore their potential of action using in vivo models, which may be contributing to the development of new antitumor drugs to be utilized in TNBC treatment. In addition, future studies can be based on employing other amine moieties featuring aromatic segments such as benzylamine and 1-naphthylamine in the structure of the SCS ligand. This may enhance the lipophilicity of compounds due to existing phenyl rings and facilitate their passage through cell membranes; consequently, promote their activity. The HOMO and LUMO analysis were used to determine the charge transfer within the compounds and the calculated HOMO and LUMO energies may reflect the chemical activity of the compounds.

### Declaration of Competing Interest

The authors declare that they have no known competing financial interests or personal relationships that could have appeared to influence the work reported in this paper.

### Acknowledgements

The authors are grateful to the Department of Chemistry, Iran University of Science and Technology (IUST), Tehran, Iran, for providing the facilities necessary for the execution of this work. The authors are also thankful to the Department of Chemistry, Université de Montreal, Montreal, Canada, for spectroscopic facilities and X ray analysis. M.H.K is appreciative for the financial support received from the Iran National Science Foundation INSF (98016046).

### Appendix A. Supplementary data

The following are available online, Experimental section containing preparation of compounds, Figures S1–S4: UV-vis spectra, packing diagrams of crystal structures, cytotoxicity and cell viability graphs related to MTT assay, Tables S1–S3: X-ray crystallographic details of  $L^1NiCl$  and  $L^1NiBr$ , selected bond lengths and angles of the crystal structures and molecular orbitals. Complete details of the X-ray analyses reported herein have also been deposited at The Cambridge Crystallographic Data Centre (CCDC 2009341 ( $L^1NiCl$ ) and 2009342 ( $L^1NiBr$ )). These data can be obtained free of charge via [www.ccdc.cam.ac.uk/data\\_request/cif](http://www.ccdc.cam.ac.uk/data_request/cif), by e-mailing [data\\_request@ccdc.cam.ac.uk](mailto:data_request@ccdc.cam.ac.uk), or by contacting The Cambridge Crystallographic Data Centre, 12, Union Road, Cambridge CB2 1EZ, U.K. (fax +44 1223 336033) Supplementary data to this article can be found online at <https://doi.org/10.1016/j.bmcl.2021.128107>.

### References

- [1] Domínguez-Martín EM, Mosteiro-Miguéns DG, Vigo-Gendré L, et al. Non-platinum metal complexes as potential anti-triple negative breast cancer agents. *Crystals*. 2018;8(10):369.
- [2] Golbaghi G, Castonguay A. Rationally designed ruthenium complexes for breast cancer therapy. *Molecules*. 2020;25(2):265.
- [3] Al-Mahmood S, Sapiezynski J, Garbuzenko OB, Minko T. Metastatic and triple-negative breast cancer: challenges and treatment options. *Drug Deliv Transl Res*. 2018;8(5):1483–1507.
- [4] Bianchini G, Balko JM, Mayer IA, Sanders ME, Gianni L. Triple-negative breast cancer: challenges and opportunities of a heterogeneous disease. *Nat Rev Clin Oncol*. 2016;13(11):674.
- [5] Mehanna J, Haddad FG, Eid R, Lambertini M, Kourie HR. Triple-negative breast cancer: current perspective on the evolving therapeutic landscape. *Int J Women's Health*. 2019;11:431.
- [6] Karginova O, Weekley CM, Raoul A, et al. Inhibition of copper transport induces apoptosis in triple-negative breast cancer cells and suppresses tumor angiogenesis. *Mol Cancer Ther*. 2019;18(5):873–885.
- [7] Işceli C, Yilmaz VT, Aygun M, Ulukaya E. Trans-Pd/Pt(II) saccharinate complexes with a phosphine ligand: Synthesis, cytotoxicity and structure-activity relationship. *Bioorg Med Chem Lett*. 2020;30(9): 127077.
- [8] Dasari S, Tchounwou PB. Cisplatin in cancer therapy: molecular mechanisms of action. *Eur J Pharmacol*. 2014;740:364–378.
- [9] Pires AS, Batista J, Murtinho D, et al. Synthesis, characterization and evaluation of the antibacterial and antitumor activity of halogenated salen copper (II) complexes derived from camphoric acid. *Appl Organomet Chem*. 2020:e5569. <https://doi.org/10.1002/aoc.5569>.
- [10] Ahir M, Bhattacharya S, Karmakar S, et al. Tailored-CuO-nanowire decorated with folic acid mediated coupling of the mitochondrial-ROS generation and miR425-PTEN axis in furnishing potent anti-cancer activity in human triple negative breast carcinoma cells. *Biomaterials*. 2016;76:115–132.
- [11] Manigandan A, Handi V, Sundaramoorthy NS, et al. Responsive nanomicellar theranostic cages for metastatic breast cancer. *Bioconjug Chem*. 2018;29(2): 275–286.
- [12] Paholak HJ, Stevers NO, Chen H, et al. Elimination of epithelial-like and mesenchymal-like breast cancer stem cells to inhibit metastasis following nanoparticle-mediated photothermal therapy. *Biomaterials*. 2016;104:145–157.
- [13] Biancalana L, Zaccini S, Ferri N, Lupo MG, Pampaloni G, Marchetti F. Tuning the cytotoxicity of ruthenium (II) para-cymene complexes by mono-substitution at a triphenylphosphine/phenoxydiphenylphosphine ligand. *Dalton Trans*. 2017;46(47):16589–16604.
- [14] Hongthong K, Ratanaphan A. BRCA1-associated triple-negative breast cancer and potential treatment for ruthenium-based compounds. *Curr Cancer Drug Targets*. 2016;16(7):606–1517.
- [15] Friks M, Martínez A, Elie BT, et al. In vitro and in vivo evaluation of water-soluble iminophosphorane ruthenium (II) compounds. A potential chemotherapeutic agent for triple negative breast cancer. *J Med Chem*. 2014;57(23):9995–10012.
- [16] Nhuquaw T, Temboot P, Hansongnern K, Ratanaphan A. Cellular responses of BRCA1-defective and triple-negative breast cancer cells and in vitro BRCA1 interactions induced by metallo-intercalator ruthenium (II) complexes containing chloro-substituted phenylazopyridine. *BMC cancer*. 2014;14(1):73.
- [17] Hearn JM, Hughes GM, Romero-Canelón I, et al. Pharmacogenomic investigations of organo-iridium anticancer complexes reveal novel mechanism of action. *Metalomics*. 2018;10(1):93–107.
- [18] Ahmad MH, Rahman NA, Kadir FA, Al-Ani LA, Hashim NM, Yehye WA. Design and synthesis of sulfur-containing butylated hydroxytoluene: antioxidant potency and selective anticancer agent. *J Chem Sci*. 2019;131(10):107.
- [19] Cerella C, Dicato M, Jacob C, Diederich M. Chemical properties and mechanisms determining the anti-cancer action of garlic-derived organic sulfur compounds. *Anti-Cancer Agents Med Chem (Formerly Current Medicinal Chemistry-Anti-Cancer Agents)*. 2011;11(3):267–271.
- [20] Hosseini-Kharat M, Rahimi R, Zargarian D, et al. Antiproliferative activity of morpholine-based compounds on MCF-7 breast cancer, colon carcinoma C26, and normal fibroblast NIH-3T3 cell lines and study of their binding affinity to calf thymus-DNA and bovine serum albumin. *J Biomol Struct Dyn*. 2019;37(14): 3788–3802.
- [21] Hosseini-Kharat M, Zargarian D, Alizadeh AM, et al. In vitro and in vivo antiproliferative activity of organo-nickel SCS-pincer complexes on estrogen responsive MCF7 and MC4L2 breast cancer cells. Effects of amine fragment substitutions on BSA binding and cytotoxicity. *Dalton Trans*. 2018;47: 16944–169557.
- [22] Prince S, Mapolie S, Blanckenberg A. *Palladium-based anti-cancer therapeutics*. *Encyclopedia of Cancer*. Springer-Verlag, Berlin Heidelberg; 2015.
- [23] Jones MM, Basinger MA, Holscher MA. Control of the nephrotoxicity of cisplatin by clinically used sulfur-containing compounds. *Toxicol Sci*. 1992;18(2):181–188.
- [24] Nojima Y, Nonoyama M, Nakajima K. Cyclopalladation of N-(p-thiolioluoil) pyrrolidine and piperidine. *Polyhedron*. 1996;15(21):3795–3809.
- [25] Pahontu E, Fala V, Gulea A, Poirier D, Tapcov V, Rosu T. Synthesis and characterization of some new Cu (II), Ni (II) and Zn (II) complexes with salicylidene thiosemicarbazones: antibacterial, antifungal and in vitro antileukemia activity. *Molecules*. 2013;18(8):8812–8836.
- [26] Agarwal RK, Singh L, Sharma DK. Synthesis, spectral, and biological properties of copper (II) complexes of thiosemicarbazones of Schiff bases derived from 4-aminoantipyrine and aromatic aldehydes. *Bioinorg Chem Appl*. 2006, ID 59509, 1–10.



- [27] Koizumi TA, Teratani T, Okamoto K, Yamamoto T, Shimoi Y, Kanbara T. Nickel (II) complexes bearing a pincer ligand containing thioamide units: comparison between SNS-and SCS-pincer ligands. *Inorg Chim Acta*. 2010;363(11):2474–2480.
- [28] Perlepes SP, Kabanos T, Hondrellis V, Tsangaris JM. The coordination chemistry of N-(2-pyridyl) pyridine-2'-carboxamide; a potentially tridentate ligand containing one secondary amide and two 2-pyridyl donor groups. *Inorg Chim Acta*. 1988;150(1):13–23.
- [29] Kanbara T, Kawai Y, Hasegawa K, Morita H, Yamamoto T. Preparation of polythioamides from dialdehydes and diamines with sulfur by the Willgerodt-Kindler type reaction. *J Polym Sci, Part A: Polym Chem*. 2001;39(21):3739–3750.
- [30] Neve F, Crispini A, Di Pietro C, Campagna S. Light-emitting cyclopalladated complexes of 6-phenyl-2, 2'-bipyridines with hydrogen-bonding functionality. *Organometallics*. 2002;21(17):3511–3518.
- [31] Ghedini M, Aiello I, La Deda M, Grisolia A. Mixed 2-phenylpyridine and 5-substituted-8-hydroxyquinolines palladium (II) complexes: new emitters in solutions at room temperature. *Chem Commun*. 2003;17:2198–2199.
- [32] Consorti CS, Ebeling G, Rodembusch F, et al. A new totally flat N(sp<sup>2</sup>)/C(sp<sup>2</sup>)/N(sp<sup>2</sup>) pincer palladacycle: synthesis and photoluminescent properties. *Inorg Chem*. 2004;43(2):530–536.
- [33] Cloutier JP, Zargarian D. Functionalization of the Aryl Moiety in the Pincer Complex (NCN)NiIIIIBr<sub>2</sub>: Insights on NiIII-Promoted Carbon-Heteroatom Coupling. 2018, 37(9), 1446–1455.
- [34] Pandarus V, Zargarian D. New pincer-type diphosphinito (POCOP) complexes of nickel. *Organometallics*. 2007;26(17):4321–4334.
- [35] Mangin LP, Zargarian D. C-H nickellation of phenol-derived phosphinites: regioselectivity and structures of cyclonickellated complexes. *Dalton Trans*. 2017; 46(46):16159–16170.
- [36] Cloutier JP, Vabre B, Moungang-Soume B, Zargarian D. Synthesis and reactivities of new NCN-type pincer complexes of nickel. *Organometallics*. 2015;34(1): 133–145.
- [37] War JA, Srivastava SK, Srivastava SD. Design, synthesis and DNA-binding study of some novel morpholine linked thiazolidinone derivatives. *Spectrochim Acta Part A Mol Biomol Spectrosc*. 2017;173:270–278.
- [38] Churushova SG, Aleksanyan DV, Rybalkina EY, et al. Highly cytotoxic palladium (II) pincer complexes based on picolinylamides functionalized with amino acids bearing ancillary S-donor groups. *Inorg Chem*. 2017;56(16):9834–9850.
- [39] Muralisankar M, Basheer SM, Haribabu J, Bhuvanesh NS, Karvembu R, Sreekanth A. An investigation on the DNA/protein binding, DNA cleavage and in vitro anticancer properties of SNO pincer type palladium (II) complexes with N-substituted isatin thiosemicarbazone ligands. *Inorg Chim Acta*. 2017;466:61–70.
- [40] Montana AM, Batalla C. The rational design of anticancer platinum complexes: the importance of the structure-activity relationship. *Curr Med Chem*. 2009;16: 2235–2260.
- [41] Sheena Mary Y, Yohannan PC, Sapnakumari M, et al. MEP analysis and molecular docking study of 1-[3-(4-Fluorophenyl)-5-phenyl-4,5-dihydro-1H-pyrazol-1-yl] ethanone. *Spectrochim Acta Part A Mol Biomol Spectrosc*. 2015;136(B):483–493.